RESEARCH PAPER

Improvement of Al-SiC Alloy Strength Through Nano-SnO2 Addition Using Powder Metallurgy Method: Study of Mechanical Properties

Khaldoon Hussein Hamzah

Department of Materials Engineering, College of Engineering, University of Al- Qadisiyah, Qadisiyyah, Iraq

ARTICLE INFO

Article History:

Received 13 May 2025 Accepted 14 September 2025 Published 01 October 2025

Keywords:

Al-SiC alloy system Material powders Metal oxide composites Metallurgy technique Tin oxide

ABSTRACT

The industrial importance of aluminum (Al) alloys has led to extensive research focused on enhancing their mechanical properties and corrosion resistance through the incorporation of nanoceramic materials. This study utilizes powder metallurgy to fabricate and reinforce an Al-SiC alloy with varying weight percentages of tin oxide (SnO₂) nanocrystalline powder at concentrations of 0, 3, 6, 9, and 12 wt%. The primary objective was to investigate the resulting mechanical and elastic properties, as well as the wear behavior of the composites. Microstructural characterization was performed using X-ray diffraction (XRD) and scanning electron microscopy (SEM). Results indicate that increasing the sintering temperature to 550 °C improved densification. The addition of 12 wt% SnO₂ significantly enhanced the material's properties, increasing microhardness, compressive strength, and Young's modulus by 162%, 146%, and 65%, respectively.

How to cite this article

Hamzah K. Improvement of Al-SiC Alloy Strength Through Nano-SnO2 Addition Using Powder Metallurgy Method: Study of Mechanical Properties. J Nanostruct, 2025; 15(4):2159-2169. DOI: 10.22052/JNS.2025.04.056

INTRODUCTION

As a result of technological developments in recent years, which have required special properties not provided by metals alone, such as high strength and corrosion resistance, researchers have considered producing metal composites consisting of a specific combination of metals to achieve special properties [1-3]. One important material in this context for use as a matrix for producing composites is aluminum composites (AMCs) reinforced with ceramic particles [4]. Aluminum alloys play an important role in many industries and technological circles, including the automotive, aerospace, and defense industries [5,6]. However, compared to Al pure and alloys have lower ductility and higher strength, making them ideal for use as a matrix [7]. Al and its alloys'

remarkable resistance to air corrosion has been demonstrated by numerous investigations to be due to their capacity to produce an oxide layer that shields them from outside effects, particularly corrosive solutions. [8-11]. By modifying the surrounding corrosive environment, various corrosion inhibitors can be applied to increase corrosion resistance. Interestingly, these inhibitors consist of alloying components and surface anodizing. Despite these distinct properties of Al alloys, aluminum nanocomposites (AMCs) are not as desirable as other homogeneous alloys [12-14]. The disadvantages of these nanocomposites include internal stress, manufacturing defects, and microstructural variations, which ultimately lead to galvanic effects. Several researchers have

^{*} Corresponding Author Email: khaldoon.hussein@qu.edu.iq

studied Al alloy matrixes. For example, Zhu et al. 2022, [15] developed an aluminum alloy coated with tin oxide (SnO₂) thin film. The results showed that adding 8% silicon carbide (SiC) particles significantly increased the tensile strength and toughness of the alloy by approximately 26% and 46%, respectively. Aluminum alloy was hand-cast with SnO₂ nanoparticles to produce nanocomposite powders with different SnO₂ concentrations. These powders were pressed and heat-treated in the presence of argon, where the increase in SnO₂ significantly improved the compressive strength and toughness of the nanocomposites [16]. There are several techniques and methods for preparing nanocomposites of Al and its alloys, such as powder metallurgy (PM) [17, 18], microagitation [19], compression casting [20], and stir casting [21]. The latter provides a homogeneous distribution of particles in the microstructure and is a modern and economical method for efficiently dispersing reinforcements into the matrix [22,23]. As a result of these significant advantages, mechanical alloying (MA) is one of the best surface treatment techniques for producing nanocomposites. This method enables control of the size and shape of the reinforcing additive. The mechanical alloying process involves crushing and welding powder particles. The process is highly dependent on important parameters such as grinding time, speed, grinding type, ball-topowder ratio (BPR), and flask/ball material [24]. Al alloys made via powder metallurgy can benefit from the addition of SnO, as a strengthening agent. Within the metal matrix, SnO₂ functions as finely dispersed reinforcing particles. Dislocations, which are flaws in the metal's crystal structure, are hampered by these particles. The alloy's strength and hardness are increased by retarding dislocation movement [25, 26]. In this work, we conducted a comprehensive investigation to improve the mechanical properties, flexibility, and resistance to wear and corrosion, by doping the Al-SiC alloy with varying weight percentages of tin oxide nanoparticles generated by the metal powder method, where mixed with different ratios of SnO₂ (3, 6, 9, and 12) wt% using powder metallurgy method.

MATERIALS AND METHODS

The matrix in this study was Al–SiC alloy, and the tin oxide nanoparticles (less than 80 nm) were reinforced with 0, 3, 6, 9, and 12 weight percent (Table 1). The Al-SiC alloy was made by the mechanical alloying process. Al (99.9%), SiC (99.9%) were the ingredients. For 24 hours, the Al alloy's constituent parts were combined in a planetary ball mill spinning at 130 rpm. These mixtures were put through a 24-hour grinding process at 500 rpm in order to create nanocomposites. The grinding procedure was done in two-hour cycles with two-hour break periods. XRD and SEM were used to characterize the mechanically cast powders in order to examine their morphology. A diffractometer was used to quantify the particle size in order to determine each powder's average distribution pattern [5]. Using the Scherrer equation, the intensity of the diffraction peaks was used to determine the crystallite size of the ground powders. After that, the powdered powders were crushed and sintered in an argon atmosphere for an hour at 550 °C. It is significant to remember that the mixing rule was used to determine the specimens' theoretical densities, accounting for the fact that the density of SnO₂ is 5.68 g/cm3 and that of the Al-SiC alloy is 2.7 g/cm3. However, the bulk density and obvious porosity were measured using the Archimedes approach. Utilising a scanning electron microscope, the microstructure of the sintered specimens was examined (SEM; Philips XL30). Shimadzu-HMV (Japan) was used to test the micro-Vickers hardness (HV) in accordance with ASTM standard B933-09, as detailed in reference [25]. Additionally, the sintered nanocomposites underwent compression testing in compliance with ASTM standard. The maximum levels of stress and strain on the stress-strain curve correlate to the ultimate strength and elongation, respectively, since the stress-strain curve was utilised to calculate the final strength, yield strength, and elongation. A pin-on-disc testing equipment was used to conduct the wear test, and a digital scale with a 0.0001 g precision was used to weigh and measure the samples. Every sample had the same size and was processed coarsely using varying grades of grinding paper (600 to 4000). Four distinct loads were used in the test. The following formulas were used to determine the wear rate brought on by weight loss [27]:

Net weight = weight befor wear - weight after wear (1)

Wear rate = net weight/time
$$(2)$$

RESULTS AND DISCUSSION

Fig. 1 displayed the XRD patterns of the ASO, AS3, AS6, AS9, and AS12 nanocomposite powders. Based on the reference card numbers (JCPDS 01-089-4037 and 96-901-2197), the primary phases of the powder are Al and SiC, respectively, as the XRD pattern of sample AZO (matrix) makes evident. XRD results showed that the characteristic aluminum peaks at angles (39.51°, 44.73°, and 65.12°) remained clearly visible with almost no change in location or intensity across all samples, indicating that the primary phase was not affected by the presence of SnO₂. Silicon carbide (SiC) peaks at angles (60.32°, 7°, and 2.64°) were also prominent and stable, reflecting its homogeneous distribution in the metal matrix [28]. However, depending on

card numbers, SnO₂ peak arise from its addition in varying amounts (JCPDS 86-1450). The results also showed that with increasing SnO₂ content, new peaks appeared at angles such as 26.61°, 33.95°, and 51.83°, attributed to the tetragonal phase of SnO₂. The gradual increase in intensity of these peaks indicates increased precipitation of this compound within the structure, without crystalline interference with other phases, indicating a phase segregation pattern. These results suggest that the increased presence of SnO2 in the form of finely dispersed particles enhances the potential for solid dispersion reinforcement, leading to improved yield strength and hardness [29]. Its presence alongside SiC also contributes to dual microstructural reinforcement, which enhances

Table 1. The Al-SiC alloy's composition after preparation.

•	The composite mixture		
Sample name —	Al-SiC alloy	SnO ₂ (wt%)	
AS0	100	0	
AS3	97	3	
AS6	94	6	
AS9	91	9	
AS12	88	12	

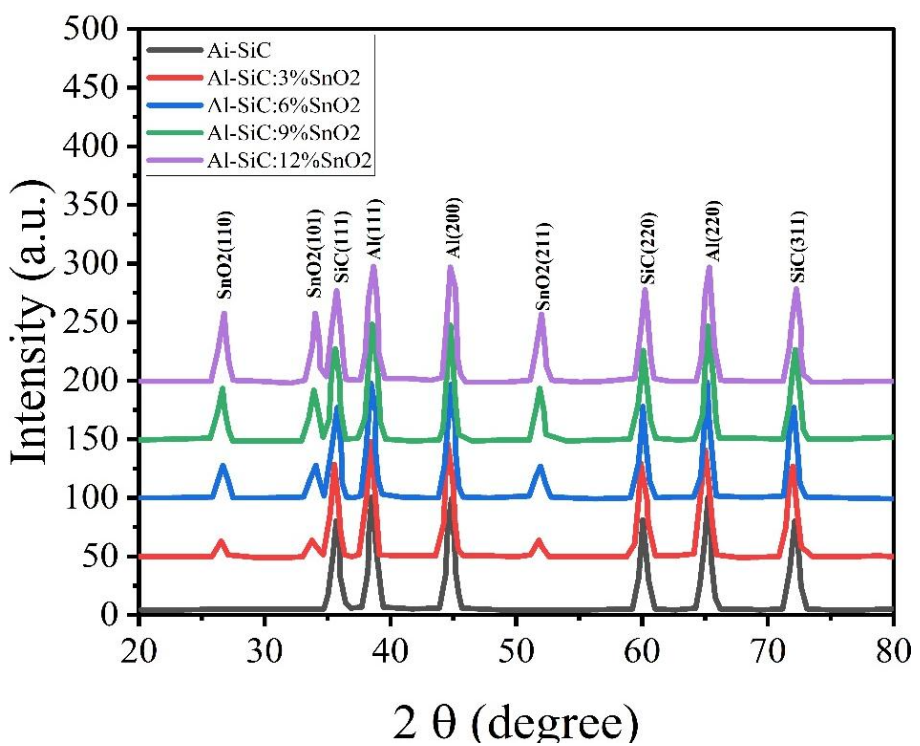


Fig. 1. XRD diagrams of Al-SiC: SnO,

the overall mechanical performance of the alloy, especially in applications requiring high corrosion resistance and hardness [30]. The results also indicate that the powder metallurgy technique allowed for the homogeneous distribution of both SiC and SnO₂ within the aluminum matrix, without the occurrence of undesirable interfacial interactions or secondary phases, enhancing the

efficiency of this method for preparing nanoscale or advanced alloys [31]. As seen in Fig. 2, it can be inferred that the breadth of the crystallite grows and its density dramatically lowers as the weight % of SnO₂ steadily increases. This results in a decrease in the size of the crystallite. Samples ASO, AS3, AS6, AS9, and AS12 have average crystallite sizes of 32.25, 31.35, 29.43, 24.99, and 19.53 nm,

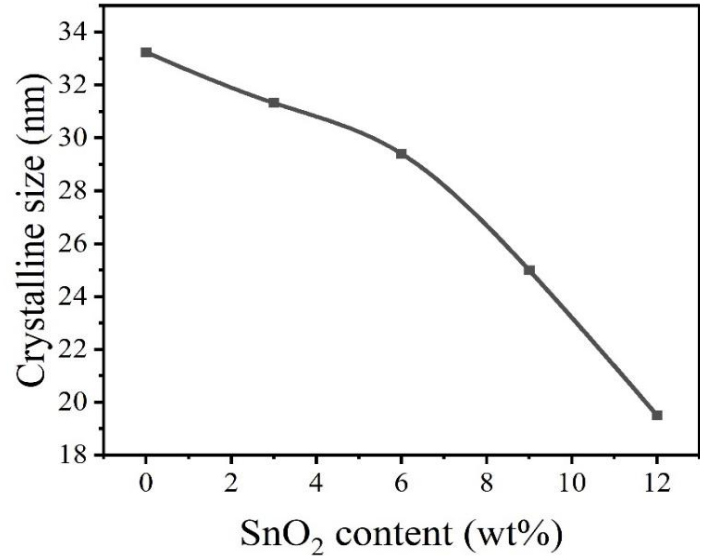


Fig. 2. Impact of SnO2 particle doping on the crystal size of powdered Al-SiC.

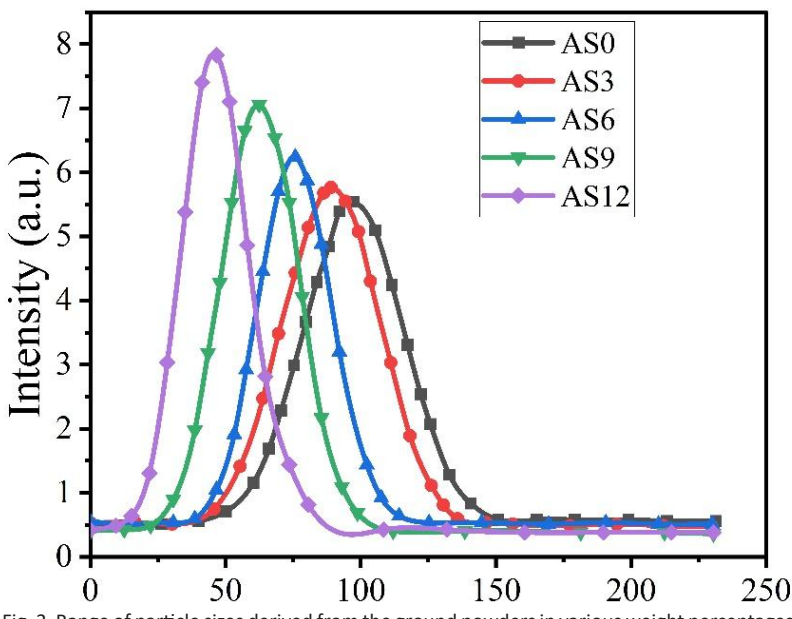


Fig. 3. Range of particle sizes derived from the ground powders in various weight percentages of SnO_3 .

respectively. These results match the results of the researcher (Özay et al., 2018) [32].

Compaction of mixed nanocomposite powders is frequently a crucial step to getting bulk materials following sample preparation. As a result, this procedure controls the final sintered compacted materials' porosity and nanoscale structure [33]. The relative intensity and obvious porosity of the felt samples after an hour at 550 °C are described in Fig. 3, which also displays the bar graph that represent the weight percentages of SnO₂. Additionally, Table 2 provides the standard deviation of the observed relative density with apparent porosity. The ASO, AS2, AS4, AS8, and AS16 samples have theoretical densities of 2.66, 2.69, 2.72, 2.78, and 2.91 g/cm³, in that order. Following sintering at 550 °C, the ASO and AS16 samples have relative densities of 93.23 and 85.97%, respectively. The compressive strength of the sintered samples with greater SnO, weight percentages may be decreased as a result of the strength of the SnO₂ ceramic particle in the Al alloy matrix. Furthermore, the SnO₂ hardener has a melting point of about 1630 °C, which is significantly higher than the Al matrixes. Therefore, the high quantities of SnO₂ act as a barrier to diffusion stages during the sintering procedure and inhibit it [34]. On the other hand, by fostering more interparticle hugs and enhancing the degree of connectedness between them, the sintering temperature of 550 °C can successfully increase the relative density. [35] The samples' relative density dropped from 97.57 to 92.12% when the SnO₂ level was increased from 0 to 12 wt% (Fig. 4).

Following 20 hours of grinding and compression at 50 MPa, SEM images of the compacted ASO, AS6, and AS12 nanocomposite powders were displayed in Fig. 5a–c. The placement of SnO₂ nanoparticles in the well-densified AI alloy matrix significantly influences the mechanical and electrical characteristics of the finished nanocomposites, according to a careful examination of the SEM

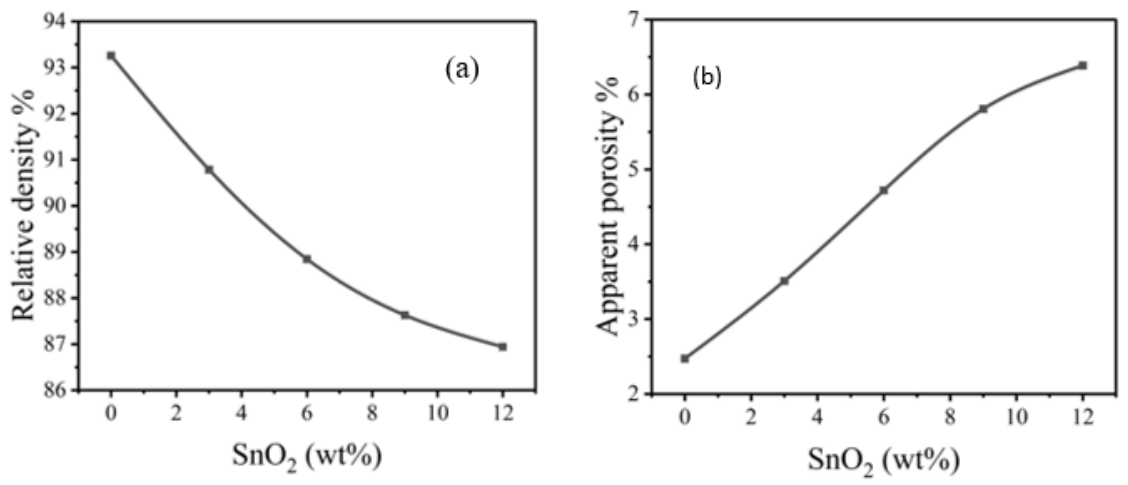


Fig. 4. The sintered samples' (a) relative density also, (b) apparent porosity.

Table 2. the apparent porosity and relative density standard deviations for each evaluated sample.

Sample name -	Stander deviation		
	Relative density %	Apparent porosity %	
AS0	0.244	0.61	
AS3	0.222	0.70	
AS6	0.218	0.88	
AS9	0.182	1.03	
AS12	0.145	1.05	

images. The SEM pictures of the nanocomposites with varying SnO_2 nanoparticle concentrations that were sintered at 550 °C were displayed in Figs 5d–f. SnO_2 nanoparticles are usually found along the matrix's grain edges in aluminum alloys. A uniform distribution of SnO_2 particles is seen in the sample with the lowest SnO_2 level; as the SnO_2 content increases, this fine distribution becomes less pronounced. As a result, the SnO_2 particle

distribution is uniform in both AS6 nanocomposite specimens but diminishes in the AS12 samples. Interestingly, in the examined samples, porosity showed the reverse pattern, rising as the quantity of SnO₂ particles increases. However, a greater densification behavior is produced, which is almost full density. The contact boundaries between the particles seem to widen through the sintering stage of the nanocomposite samples, suggesting

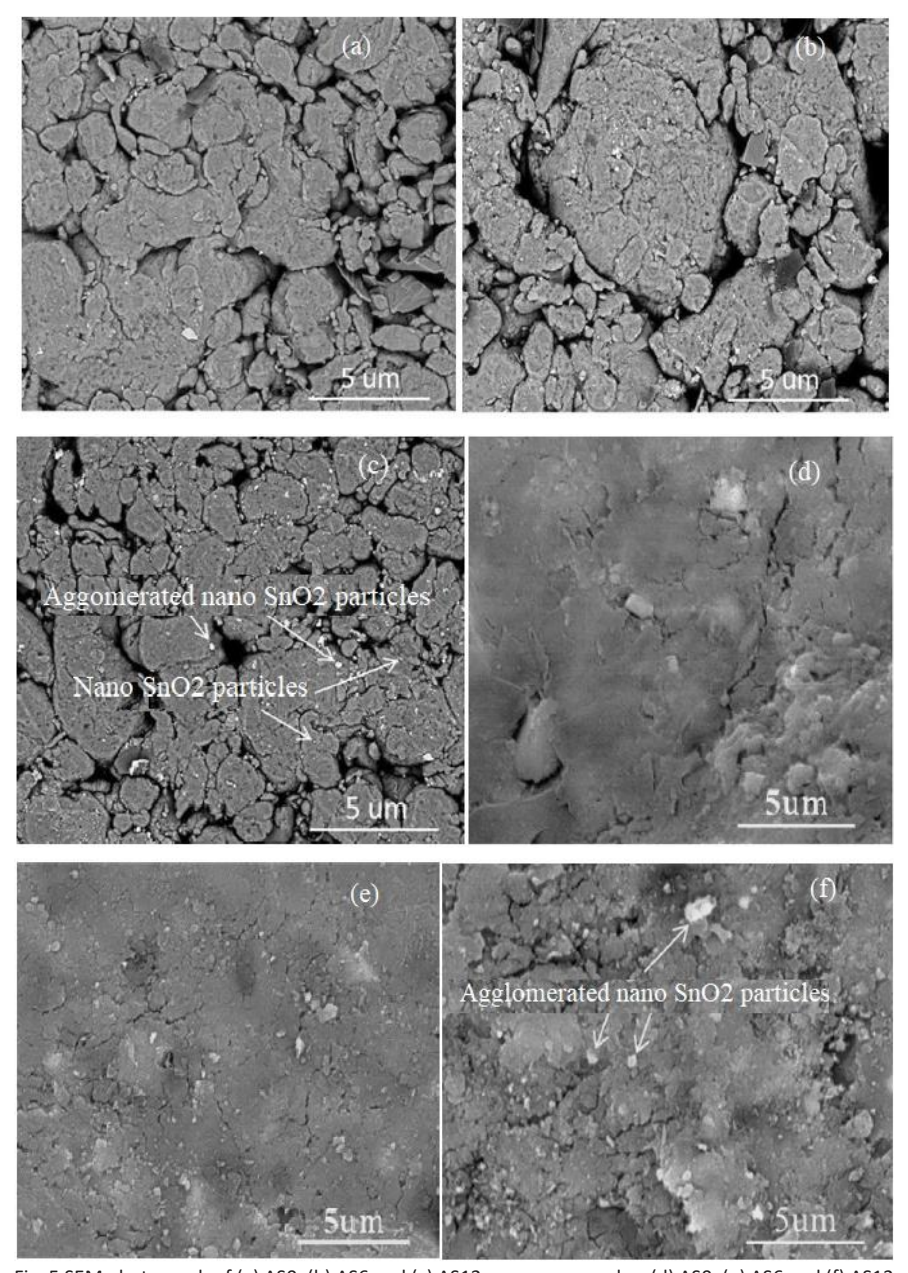
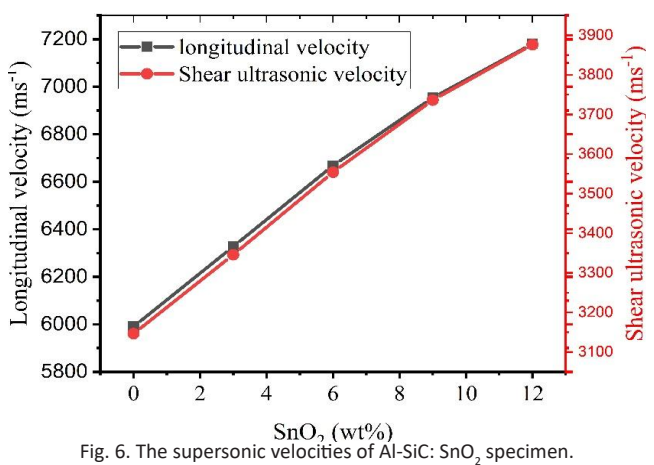


Fig. 5 SEM photograph of (a) ASO, (b) AS6 and (c) AS12 compose samples, (d) ASO, (e) AS6 and (f) AS12 samples sintered at 550 °C.

that a strong binding between the nanocomposite matrix and SnO₂ was achieved and that there were no holes in the SnO₂ particle area [36]. These results match the results of the researcher Lai et al., 2021 [37].

Non-destructive ultrasonic technology (NDT) was used to assess the longitudinal (VL) and cut (VS) ultrasonic quickness of the sintered samples at 550°C (Fig. 6). It is important to note that increased ultrasonic velocities result from raising the SnO,



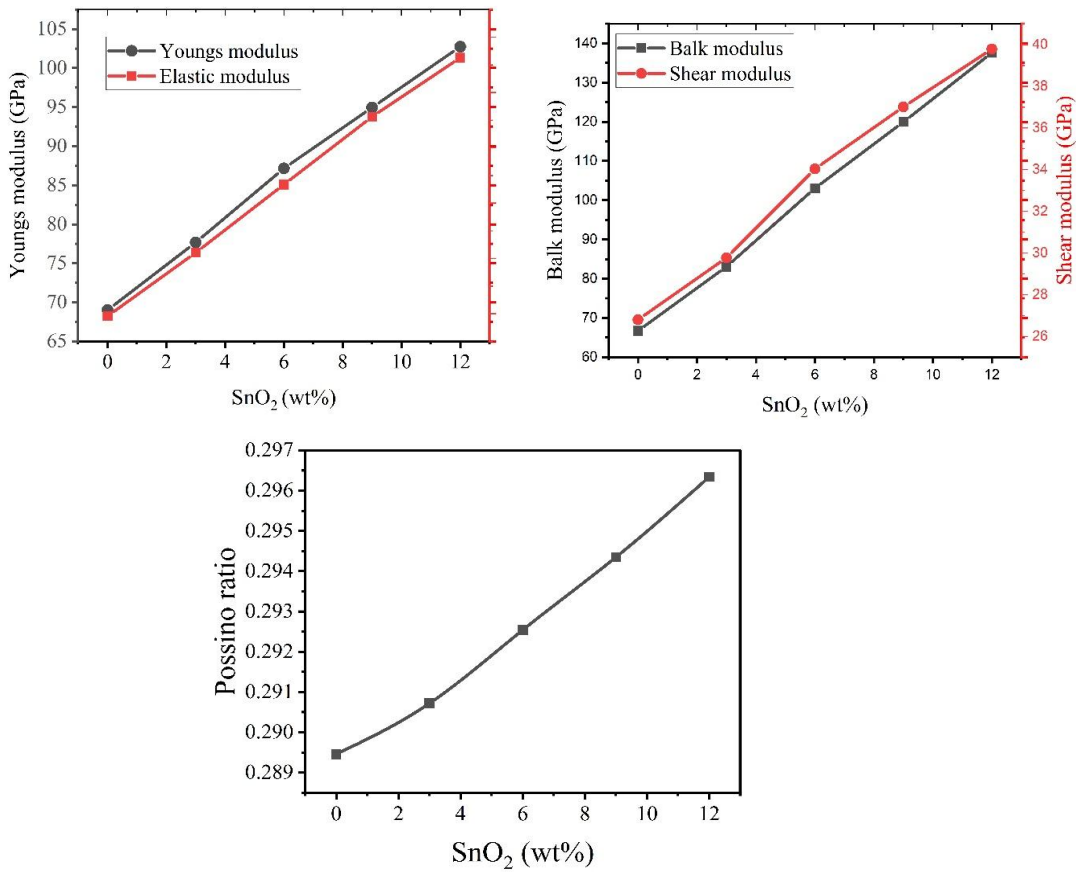


Fig. 7. The collection of elastic moduli of Al-SiC: SnO₂ specimen.

concentration from 3 to 12 weight percent. The findings indicate that when the quantity of SnO₃ increased, the specimen VL and VS amount varied from 5886.5 to 7510.3 and 3205.7 to 4027.3 ms⁻¹, respectively. Fig. 7 shows the elastic moduli of the nanocomposites under investigation. The figure shows that, in relation to the ultrasonic velocities, the elastic moduli exhibit a similar pattern [38]. For instance, the ASO sample has an elastic modulus of 89.7 and a Poisson's ratio of 0.2896 GPa. Interestingly, after adding 12% SnO₂, they rose to 150.6 GPa and 0.2983 GPa, respectively. In complete agreement with the accurate results for microhardness and strength of compressive, the inclusion of SnO, nanoparticles as reinforcement greatly increased the elastic moduli and ultrasonic speeds. These results match the results in the same line of the researcher Khan et al.,2024. [39].

Fig. 8 shows the average microhardness (HV) values of Al-SiC alloy and Al-SiC: SnO. nanocomposite samples that were annealed at 550°C. As the quantity of different SnO, particles of Al alloy matrix high, the findings demonstrate a considerable increase in microhardness values. The microhardness of the Al alloy matrix increases from 431.13 to 1124.6 MPa with the addition of 12 weight percent SnO₂. The enhanced microhardness of the nanocomposite specimens can be attributed to a number of factors, including the presence of ceramic parts, the even distribution of reinforce

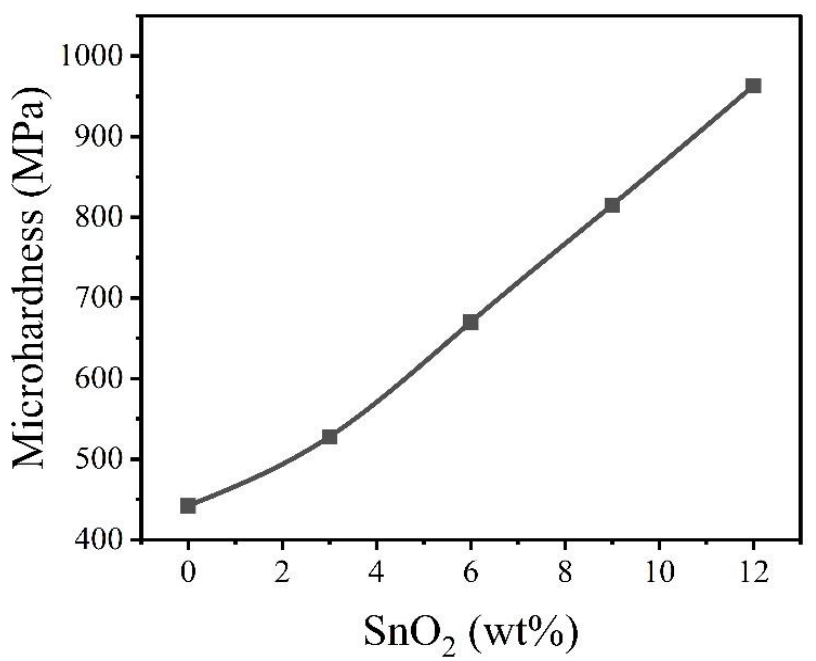


Fig. 8. Microhardness of Al-SiC: SnO₂ samples.

Table 3. Standard deviation of wear rate for (Al-SiC): SnO₂ specimen.

Samples -	Stander deviation			
	10 N	20 N	40 N	
AS0	0.00071	0.0004	0.00054	
AS3	0.00054	0.00068	0.00056	
AS6	0.00076	0.0006	0.00044	
AS9	0.00087	0.0003	0.00032	
AS12	0.00049	0.00068	0.00038	



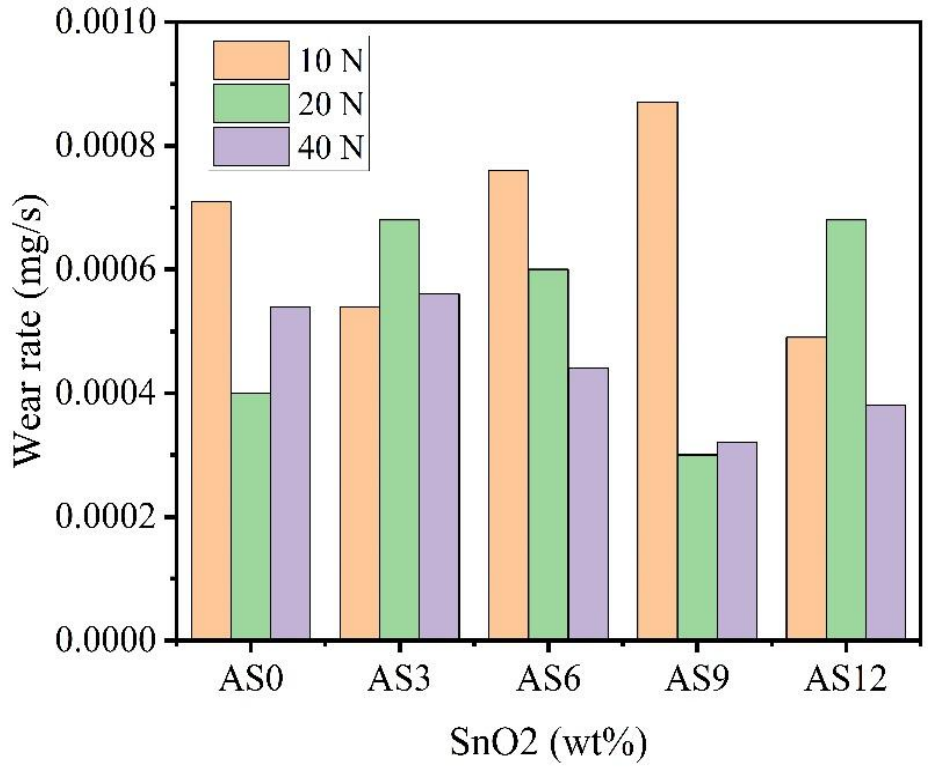


Fig. 9. Wear rate of sintered (Al-SiC): SnO₂ samples at (10, 20, 40) N loads.

within the matrix, and the Al alloy matrix's decreasing grain sizes as the concentration of SnO₂ increases [39].

A histogram plot of the wear rates of ASO, AS3, AS6, AS9, and AS12 samples under loads of 10, 20, and 40 N is displayed in Fig. 9. The standard deviation of the observed wear rates is also displayed in Table 3 The results show that although the nanocomposite samples' wear resistance tends to increase with increasing SnO₂ concentrations, it tends to deteriorate with increasing load [40, 41]. An unreinforced sample (ASO) will corrode at rates of 0.01 g/s, 0.0084 g/s, and 0.0126 g/s when stresses of 10, 20, and 40 N are applied.

CONCLUSION

In this study, SnO_2 nano powder and Al-SiC alloy nanocomposites were made via powder metallurgy. The study's conclusions were as follows:

1. The findings demonstrated that the produced nanocomposites had observable agglomerations and a uniform dispersion of tin oxide nanoparticles inside the alloy matrix.

- 2. As the amount of tin oxide particles increased, the particle size shrank until it reached 45.9 nm for the sample that included 12% tin oxide by weight.
- 3. As the quantity of tin oxide in the samples grew, the obvious porosity increased but the relative density dropped.
- 4. As the quantity of tin oxide grew, so did the elastic modulus. The bulk and elastic modulus increased to 71% and 69%, respectively, with the addition of 12% tin oxide by weight.
- 5. The microhardness, ultimate strength, and yield strength all rose in proportion to the quantity of tin oxide. The AS12 sample's maximum microhardness and ultimate strength values were approximately 1.9 and 2.2 times more than the AS0 sample's, respectively.
- 6. Wear rates in the sample rose as the load increased, but they fell as the SnO₂ level rose.

CONFLICT OF INTEREST

The authors declare that there is no conflict of interests regarding the publication of this manuscript.

REFERENCES

- Ateş S, Coşman S. Hardness, wear and thermal properties of SiC/carbon black-reinforced al6061 matrix composites produced via powder metallurgy. Science of Sintering. 2025(00):16-16.
- Moustafa EB, Abushanab WS, Ghandourah EI, Taha MA, Mosleh AO. Advancements in Surface Reinforcement of AA2024 Alloy Using Hybridized Niobium Carbide and Ceramics Particles via FSP Technique. Metals and Materials International. 2023;30(3):800-813.
- Moustafa EB, Melaibari A, Alajlani F. Enhancing tribological, mechanical, and microstructural properties of AA6061 composites with ceramic reinforcements (CrC, NbC, TaC) through friction stir processing. Journal of Materials Science. 2024;59(31):14339-14353.
- Jafarzadeh K, Ashlaghi HA, Alizadeh A, Abbasi HM. An investigation on the corrosion behaviour of B4C-reinforced AA5083 aluminium alloy in sodium chloride solution using electrochemical impedance spectroscopy. Bull Mater Sci. 2024;47(3).
- AbuShanab WS, Moustafa EB, Ghandourah E, Taha MA. Effect
 of graphene nanoparticles on the physical and mechanical
 properties of the Al2024-graphene nanocomposites
 fabricated by powder metallurgy. Results in Physics.
 2020:19:103343.
- Aydın F. A review of recent developments in the corrosion performance of aluminium matrix composites. J Alloys Compd. 2023:949:169508.
- Moustafa EB, Abdel Aziz SS, Taha MA, Saber A-H. Influence of Graphene and Silver Addition on Aluminum's Thermal Conductivity and Mechanical Properties Produced by the Powder Metallurgy Technique. Metals. 2023;13(5):836.
- Chandla NK, Kant S, Goud MM. A review on mechanical properties of stir cast Al-2024 metal matrix composites. Advances in Materials and Processing Technologies. 2022;9(3):948-969.
- Lai T, Yin Z, Shen J, Sun P, Liu Q, Wang K, et al. Effects of SnO₂
 Passive Film and Surface Micro-Galvanic Corrosion on the
 Corrosion Behavior of as-Extruded Mg-9Li-5Al-xSn Alloys. J
 Electrochem Soc. 2021;168(8):081502.
- Moustafa EB, Taha MA. Preparation of high strength graphene reinforced Cu-based nanocomposites via mechanical alloying method: microstructural, mechanical and electrical properties. Appl Phys A. 2020;126(3).
- Varol T, Hacısalihoğlu İ, Kaya G, Güler O, Yıldız F, Aksa HC, et al. The Effect of Selective Laser Melting Process on the Microstructure, Density, and Electrical Conductivity of Silver-Coated Copper Cores. J Mater Eng Perform. 2021;30(7):5216-5226.
- Moustafa EB, AbuShanab WS, Ghandourah E, Taha MA. Microstructural, mechanical and thermal properties evaluation of AA6061/Al₂O₃-BN hybrid and mono nanocomposite surface. Journal of Materials Research and Technology. 2020;9(6):15486-15495.
- 13. Li X, Nurtilek MU, Zhang Z, Wang L, Wu Q, Mao P, et al. Properties of Casting Al-Cu Alloy Modified by Mixed Rare Earth (La, Ce) and its Mechanism Analyzed. Archives of Foundry Engineering. 2024.
- Khan MA, Usman M, Zhao Y. First Principles Calculations for Corrosion in Mg-Li-Al Alloys with Focus on Corrosion Resistance: A Comprehensive Review. Computers, Materials and Continua. 2024;81(2):1905-1952.
- 15. Zhu J, Han J, Yu W, Geng N, Wan Y, Peng Y, et al. Electrodeposited SnO_/graphene composite as highly

- effective and stable anticorrosion coating for aluminum alloys in acidic environments. International Journal of Electrochemical Science. 2022;17(10):221054.
- 16. Hu J, Wang XF, Liu GY. Effect of SnO₂ coating on the damping capacity and tensile property of alumina borate whiskerreinforced aluminum composite at room temperature. Materials Science and Engineering: A. 2010;527(3):657-662.
- 17. Moustafa EB, Taha MA. The Effect of Mono and Hybrid Additives of Ceramic Nanoparticles on the Tribological Behavior and Mechanical Characteristics of an Al-Based Composite Matrix Produced by Friction Stir Processing. Nanomaterials. 2023;13(14):2148.
- Baliarsingh SS, Tripathy AG, Sahoo BP, Das D, Behera RR, Satpathy MP, et al. Comprehensive review on fabrication methods of metal matrix composites and a case study on squeeze casting. Advances in Materials and Processing Technologies. 2023;10(4):2862-2885.
- Kumar J, Singh D, Kalsi NS. A Critical Review of Fabrication Techniques and Possible Interfacial Reactions of Silicon Carbide Reinforced Aluminium Metal Matrix Composites. Metal Matrix Composites: A Modern Approach to Manufacturing: Bentham Science Publishers; 2024. p. 42-90.
- Annapoorna K, Ananda R, Deshpande V, Shobha R. Nano reinforced aluminium based Metal Matrix Hybrid Composites - an overview. Journal of Physics: Conference Series. 2024;2748(1):012007.
- Mishra RR, Panda A, Sahoo AK, Kumar R. Characterization and machinability analysis of aluminium-based metal matrix composites (MMC): A critical review. Proceedings of the Institution of Mechanical Engineers, Part C: Journal of Mechanical Engineering Science. 2024;239(3):861-884.
- 22. Gupta M, T AK. Aluminum Metal Matrix and Magnesium Metal Matrix Composites: An Insight into Processing Influences on Corrosion Properties for use in Environment-Sensitive Applications. Advanced Materials for Emerging Applications (Innovations, Improvements, Inclusion and Impact): Bentham Science Publishers; 2024. p. 252-274.
- 23. Bharat N, Jain R, Bose PSC, Kumar V. A review on fabrication and mechanical characterization of high-strength 7xxx series aluminum alloys reinforced with ceramic reinforcements. Proceedings of the Institution of Mechanical Engineers, Part N: Journal of Nanomaterials, Nanoengineering and Nanosystems. 2025.
- 24. Kumar Sharma N, Singh Rana A. Structure-Property Correlations in Metal Matrix Composites. Metal Matrix Composites: A Modern Approach to Manufacturing: BENTHAM SCIENCE PUBLISHERS; 2024. p. 18-41.
- Zhao PT, Wang LD, Du ZM, Xu SC, Jin PP, Fei WD. Low temperature extrusion of 6061 aluminum matrix composite reinforced with SnO2-coated Al18B4O33 whisker. Composites Part A: Applied Science and Manufacturing. 2012;43(1):183-188.
- Mozaffari N, Solaymani S, Achour A, Kulesza S, Bramowicz M, Nezafat NB, et al. New Insights into SnO₂/Al₂O₃, Ni/Al₂O₃, and SnO₂/Ni/Al₂O₃ Composite Films for CO Adsorption: Building a Bridge between Microstructures and Adsorption Properties. The Journal of Physical Chemistry C. 2020;124(6):3692-3701.
- 27. Alsoruji G, Moustafa EB, Alzahrani MA, Taha MA. Preparation of Silicon Bronze-Based Hybrid Nanocomposites with Excellent Mechanical, Electrical, and Wear Properties by Adding the Ti3AlC2 MAX Phase and Granite Via Powder Metallurgy. Silicon. 2022;15(6):2753-2763.



- 28. Jiju KB, Selvakumar G, Ram Prakash S. Study on preparation of AI – SiC metal matrix composites using powder metallurgy technique and its mechanical properties. Materials Today: Proceedings. 2020;27:1843-1847.
- 29. Qi D, Li G, Han X, Fang X, Feng W, Tian R. Effect of the insitu formed CuO additive on the fracture behaviour and failure mechanism of Ag-SnO₂ composites. Eng Fract Mech. 2023;284:109240.
- Wang J, Zhou X, Lu L, Li D, Mohanty P, Wang Y. Microstructure and properties of Ag/SnO2 coatings prepared by cold spraying. Surf Coat Technol. 2013;236:224-229.
- 31. Taha MA, Zawrah MF, Abomostafa HM. Fabrication of Al/ Al₂O₃/ SiC/graphene hybrid nanocomposites from Aldross by powder metallurgy: Sinterability, mechanical and electrical properties. Ceram Int. 2022;48(14):20923-20932.
- 32. Özay Ç, Gencer EB, Gökçe A. Microstructural properties of sintered Al–Cu–Mg–Sn alloys. J Therm Anal Calorim. 2018;134(1):23-33.
- Elmahdy M, Abouelmagd G, Mazen AAE. Microstructure and Properties of Cu-ZrO₂ Nanocomposites Synthesized by in Situ Processing. Materials Research. 2017;21(1).
- 34. Ağaoğulları D. Effects of ZrC content and mechanical alloying on the microstructural and mechanical properties of hypoeutectic Al-7 wt.% Si composites prepared by spark plasma sintering. Ceram Int. 2019;45(10):13257-13268.
- 35. Wahi A, Muhamad N, Sulong AB, Ahmad RN. Effect of Sintering Temperature on Density, Hardness and Strength

- of MIM Co30Cr6Mo Biomedical Alloy. Journal of the Japan Society of Powder and Powder Metallurgy. 2016;63(7):434-437
- 36. Dai S, Bian Z, Wu W, Tao J, Cai L, Wang M, et al. The role of Sn element on the deformation mechanism and precipitation behavior of the Al–Cu–Mg alloy. Materials Science and Engineering: A. 2020;792:139838.
- 37. Yin Z, He R, Chen Y, Yin Z, Yan K, Wang K, et al. Effects of surface micro–galvanic corrosion and corrosive film on the corrosion resistance of AZ91–xNd alloys. Appl Surf Sci. 2021;536:147761.
- 38. Patra A. Synthesis of Oxide Dispersion Strengthened Refractory Alloys. Oxide Dispersion Strengthened Refractory Alloys: CRC Press; 2022. p. 77-89. http://dx.doi.org/10.1201/9781003201007-4
- Li X, Liu S, Du Y. Investigation on the corrosion resistance of the Mg-10Al-xMn alloys based on thermodynamic calculations. Corros Sci. 2021;189:109631.
- Banerjee S, Robi PS, Srinivasan A, Lakavath PK. Effect of trace additions of Sn on microstructure and mechanical properties of Al–Cu–Mg alloys. Materials and Design. 2010;31(8):4007-4015.
- 41. Sadawy M, Metwally H, Abd El-Aziz H, Adbelkarim A, mohrez W, Mashaal H, et al. The role of Sn on microstructure, wear and corrosion properties of Al-5Zn-2.5Mg-1.6Cu-xSn alloy. Materials Research Express. 2022;9(9):096507.